

Localized Superconductivity in the Quantum-Critical Region of the Disorder-Driven Superconductor-Insulator Transition in TiN Thin Films

T. I. Baturina^{1,2}, A. Yu. Mironov^{1,2}, V. M. Vinokur³, M. R. Baklanov⁴, and C. Strunk²

¹*Institute of Semiconductor Physics, 630090, Novosibirsk, Russia*

²*Institut für experimentelle und angewandte Physik,
Universität Regensburg, D-93025 Regensburg, Germany*

³*Materials Science Division,
Argonne National Laboratory, Argonne, IL 60439, USA*

⁴*IMEC, Kapeldreef 75, B-3001 Leuven, Belgium*

(Dated: February 8, 2022)

We investigate low-temperature transport properties of thin TiN superconducting films in the vicinity of the disorder-driven superconductor-insulator transition. In a zero magnetic field, we find an extremely sharp separation between superconducting and insulating phases, evidencing a direct superconductor-insulator transition without an intermediate metallic phase. At moderate temperatures, in the insulating films we reveal thermally activated conductivity with the magnetic field-dependent activation energy. At very low temperatures, we observe a zero-conductivity state, which is destroyed at some depinning threshold voltage V_T . These findings indicate formation of a distinct collective state of the localized Cooper pairs in the critical region at both sides of the transition.

An early suggestion that tuning disorder strength can cause a direct superconductor-insulator transition (SIT) in two-dimensional systems [1] triggered explosive activity in experimental studies of superconductor films [2]. Experimentally, the SIT can be induced by decreasing the film thickness [3] and/or, close to the critical thickness, also by the magnetic field [4]. These scenarios are commonly referred to as disorder-driven SIT (D-SIT) and magnetic-field driven SIT. Recent studies on the B -induced insulator revealed several striking features: a magnetic-field-dependent thermally activated behavior of the conductivity [5] and a threshold response to the dc voltage [6], indicating the possible formation of a distinct collective insulating state. Importantly, these findings refer to the films belonging to the superconducting side of the D-SIT. This rises the question of whether the above findings are specific only to the superconducting side of the D-SIT or a characteristic feature of the whole critical region including both the insulating and superconducting sides of the D-SIT.

In this Letter we focus on the insulating side of the disorder-driven superconductor-insulator transition in TiN films. The transition itself turns out to be exceptionally sharp. At zero and low magnetic fields we find thermally activated behavior of the conductivity. A positive magnetoresistance and a distinct threshold behavior in the low-temperature I - V characteristics persist on the *insulating* side of the D-SIT. Our results clearly indicate that, in the vicinity of the D-SIT, the response to applied magnetic and/or electric fields, is the same irrespective of whether the underlying ground state is superconducting or insulating.

The 5-nm thick TiN films were grown by atomic layer chemical vapor deposition onto a Si/SiO₂ substrate. The samples for transport measurements were patterned into Hall bridges using conventional UV lithography and sub-

sequent plasma etching. To increase sheet resistances (R_{\square}) without introducing structural changes, the films were thinned by an additional soft plasma etching. Electron transmission micrographs and diffraction patterns revealed a polycrystalline structure in both initial and etched films, the interfaces separating densely-packed crystallites being 1–2 atomic layers thick. As we found before [7], in such samples $k_F\ell \simeq 1$, where k_F is the Fermi vector, and $\ell \sim 0.3$ nm is the mean free path. This short mean free path can be related to the enhanced Cl content (up to 3%), characteristic of films grown by the above method [8]. Four-probe resistance measurements were carried out by the standard low frequency (0.4–2 Hz) ac lock-in current source technique with the ac current 0.01–1 nA. In cases where the resistances were too high to employ the current source four-probe lock-in measurements, the two-probe voltage source technique with the ac voltage 10–30 μ V was used. At resistances $R > 1$ M Ω , this allowed us to keep the power dissipation below 10^{-15} W, thus ensuring linear regime and excluding overheating. Two-probe differential conductance vs dc voltage measurements were done by means of the low frequency ac lock-in technique combined with the dc voltage excitations. Magnetic fields up to 16 T were applied perpendicular to the film surface.

We start with the zero magnetic-field results. Figure 1(a) shows the temperature dependence of $\log R_{\square}$ for seven different films. An increase in disorder results in a growth of R_{\square} and reduces the superconductor critical temperature monotonically. We did not detect any sign of the reentrant behavior or a kink in $R(T)$, which are characteristic to the granular films and/or the films containing large scale inhomogeneities [9]. It indicates that our films do not have a granular structure but are rather homogeneously disordered. To characterize the behavior on the nonsuperconducting side, we replot the data

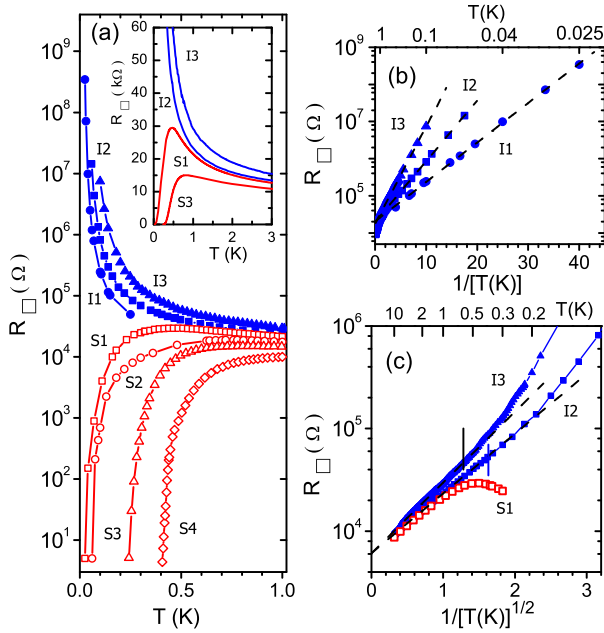


FIG. 1: (color online). Temperature dependences of R_{\square} taken at zero magnetic field for the samples near the localization threshold. (a) $\log R_{\square}$ versus T . Inset: some part of the R_{\square} data in a linear scale. (b) $\log R_{\square}$ versus $1/T$ for samples I1, I2, and I3. Dashed lines represent Eq. (1) and fit perfectly at low temperatures. All curves saturate at the same $R_{\square} \approx 20 \text{ k}\Omega$ at high temperatures. (c) R_{\square} versus $1/T^{1/2}$; dashed lines are given by $R_{\square} = R_1 \exp(T_1/T)^{1/2}$ which (with $R_1 \sim 6 \text{ k}\Omega$) will fit the data at high temperatures. Vertical strokes mark T_0 , determined by the fit to the Arrhenius formula of Eq. (1).

for R_{\square} versus $1/T$ in Fig. 1(b). At low temperatures we observe an Arrhenius behavior of the resistance, demonstrating that these samples are indeed insulators. The dashed lines correspond to

$$R = R_0 \exp(T_0/T). \quad (1)$$

The activation temperatures T_0 in the three samples measured are $T_0 = 0.25 \text{ K}$ (I1), 0.38 K (I2), and 0.61 K (I3) (the growth in T_0 corresponds to increasing disorder). The prefactor R_0 determined from the extrapolation of the dashed lines in Fig. 1(a) towards $1/T = 0$ is almost the same ($\approx 20 \text{ k}\Omega$) for all samples. Figure 1 shows that our TiN films demonstrate an abrupt switch between the superconducting and insulating phases: indeed, the “last” superconducting and the “first” insulating films are practically indistinguishable by their resistances at temperatures higher than 1 K , for instance, at $T = 10 \text{ K}$ $R_{\square} = 8.74 \text{ k}\Omega$ (S1) and $R_{\square} = 9.16 \text{ k}\Omega$ (I2). However, at lower temperatures they choose unequivocally between either the superconducting or insulating ground states.

We point out that the separatrix between the sets of “superconducting” and “insulating” $R(T)$ curves is not simply a horizontal line [$R(T) = \text{const}$]. To demonstrate that, we replot the data in the linear scale in the inset to

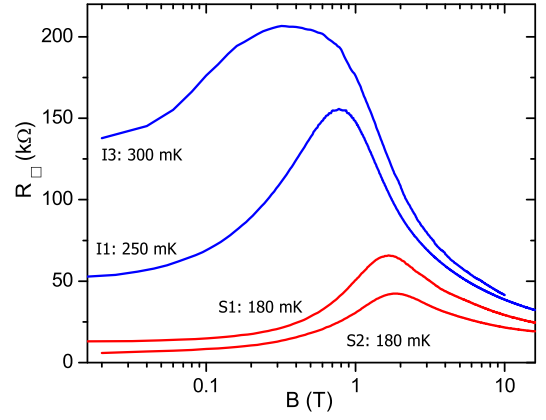


FIG. 2: (color online). Magnetoresistance isotherms for superconducting (S1, S2) and insulating samples (I1, I3) at similar temperatures. All curves converge above 2 T .

Fig. 1(a) and note that $R(T)$ dependences of superconducting samples are nonmonotonic. They exhibit an “insulating trend,” i.e. an upward turn of the resistance preceding its eventual drop to zero at low temperatures. Further insight into the evolution of TiN films across the D-SIT is drawn from the $\log R_{\square}$ against $1/T^{1/2}$ plots shown in Fig. 1(c). At $T > T_0$, the resistances of the insulating samples compare favorably with the Efros-Shklovskii (ES) formula, $R = R_1 \exp(T_1/T)^{1/2}$, [10, 11]. The temperatures T_1 in the three samples shown in Fig. 1(c) are $T_1 = 1.75 \text{ K}$ (S1), 1.80 K (I2), and 2.53 K (I3). The prefactor R_1 is again nearly the same for all samples, but in this case it is close to the quantum resistance for pairs, $h/(2e)^2 = 6.45 \text{ k}\Omega$. At lower temperatures $R(T)$ deviates from the ES behavior, which in the insulating samples turns into the Arrhenius law below T_0 , while the superconducting samples fall into a superconducting state.

Turning to the magnetoresistance data shown in Fig. 2, we see that in all samples, including the insulating films, $R(B)$ varies nonmonotonically with B . It exhibits a positive magnetoresistance (PMR) at low fields, then reaches a maximum, followed first by a rapid drop, and eventually saturates at higher magnetic fields [12], where the difference between insulating and superconducting samples is suppressed and all curves converge. Since PMR in superconducting films appears because of the suppression of superconducting phase coherence by the magnetic field, one can conjecture that this phase coherence persists also in *insulating* films. At low temperature the ratio of the magnitude of the resistance at maximum to its value at zero magnetic field increases. Figure 3 presents $R(B)$ of the sample I1 at low temperatures and shows that the resistance at low fields again follows the Arrhenius behavior with B -dependent T_0 [Eq.(1)]. The activation temperature $T_0(B)$ qualitatively follows the magnetoresistance.

We now discuss the most intriguing feature, a de-

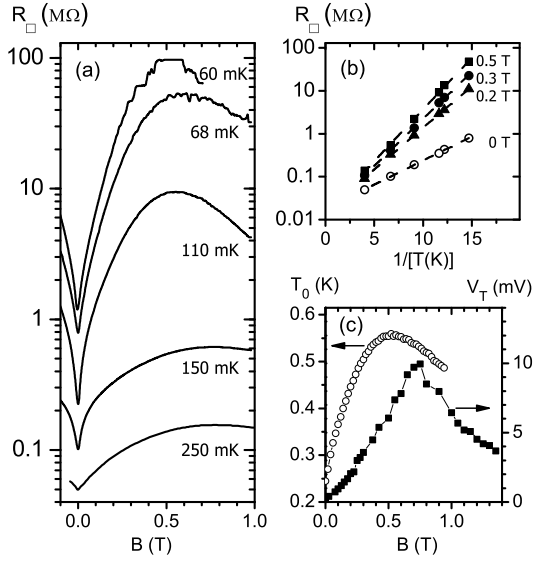


FIG. 3: (a) Sheet resistance of sample I1 as a function of the magnetic field at some temperatures listed. (b) R versus $1/T$ at $B = 0$ (open circles), 0.2 (triangles), 0.3 (filled circles), and 0.5 T (squares). The dashed lines are given by Eq. (1). (c) T_0 (left axis), calculated from fits to Eq. (1), and the threshold voltage V_T (right axis) as a function of B .

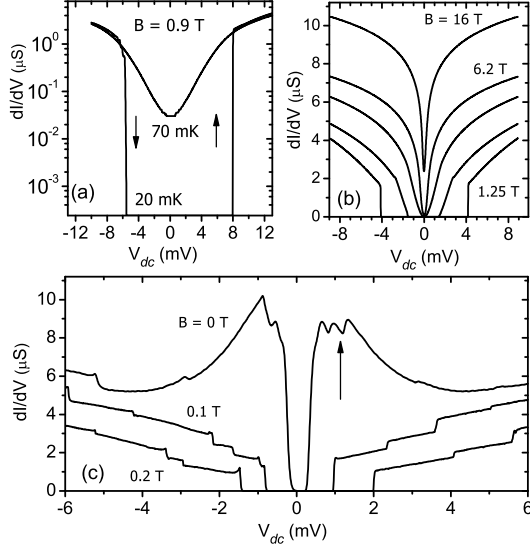


FIG. 4: Differential conductance vs dc voltage for sample I1. (a) $dI/dV(V_{dc})$ at $B = 0.9$ T at two temperatures $T = 0.02$ and 0.07 K. An arrow shows the direction of the voltage sweep. (b) $dI/dV(V_{dc})$ at $B = 1.25, 1.65, 2.7, 6.2,$ and 16 T at $T = 0.02$ K. (c) $dI/dV(V_{dc})$ at $B = 0, 0.1,$ and 0.2 T at $T = 0.02$ K.

pinning transition observed at low temperatures in the insulating films. Figure 4 reveals an abrupt onset of finite conductivity as the bias voltage V_{dc} exceeds a threshold voltage V_T : panel (a) presents a differential conductance, dI/dV versus V_{dc} measured on sample I1 at $B = 0.9$ T, using the two-probe technique with the

contact separation 1.5 mm. Two traces represent data taken at $T = 70$ mK and at the lowest temperature, $T = 20$ mK, achieved in the experiment. The dI/dV curve at $T = 70$ mK is typical for an insulator with activated conductance, showing a gradual increase of dI/dV with V_{dc} , and is symmetric with respect to the direction of the V_{dc} sweep. However, as temperature is decreased to $T = 20$ mK the voltage response changes dramatically. Under low V_{dc} , both, the current and dI/dV are immeasurably small. As soon as V_{dc} reaches some well-defined threshold value V_T , dI/dV abruptly jumps up by several orders of magnitude. The threshold behavior is accompanied by a hysteresis. A sharp conductance jump is observed up to $B \sim 2$ T. A non-Ohmic behavior remains even at $B = 16$ T. The threshold voltage changes non-monotonically upon magnetic field [see $V_T(B)$ along with $T_0(B)$ in Fig. 3(c)]. Note the large magnitude of threshold voltage to activation energy ratio: $eV_T/k_B T_0 \approx 220$ at $B = 0.7$ T.

Notable is also the nonmonotonic behavior of $dI/dV(V_{dc})$ at $B = 0$, which is displayed in Fig. 4(c). Similar to the depinning-like behavior at finite magnetic field in Figs. 4(a) and (b), we find a steep initial increase of $dI/dV(V)$ with a maximum around $V_{dc} = 1$ mV (marked by an arrow), followed by a gradual decrease. At the peak, dI/dV is about twice larger than at $V_{dc} = 4$ mV. This feature cannot be explained by electron heating and vanishes already at $B = 0.025$ T. Such a suppression of the conductivity by the bias current or voltage is typical for a superconductor in a fluctuation regime. The observation a similar “superconducting trend” in the insulating regime indicates that superconducting correlations survive also on the insulating side of the D-SIT. This implies the presence of the localized Cooper pairs and local superconducting phase coherence.

To summarize the essential findings in the D-SIT critical region, we note that the search for a disorder-driven superconductor-insulator transition has included many materials, e.g., Bi [3], MoSi [13], Ta [14], InO_x [5, 15, 16], and Be [17]. However, the immediate onset of exponential temperature dependence of the resistance, which conclusively evidences the direct transition into an insulator, was found so far only in InO_x [5, 15, 16] and Be [17] films. In Bi, MoSi, and Ta compounds [3, 13, 14] a weak logarithmic temperature dependence of the resistance was observed on the nonsuperconducting side, either because of a possible intermediate metallic phase or since the transition to the superconducting state occurs there at much lower temperatures. Our data on TiN unambiguously show a direct D-SIT with the *nonhorizontal* $R(T)$ separatrix between the insulating and superconducting sides. An insulating trend (i.e. the upturn of the separatrix) can also be seen in the data on InO_x [15] and Be [18] films. This implies that D-SIT *cannot* be described by a single-parameter scaling with the universal resistance at the transition.

The next important feature is that in all three materials exhibiting D-SIT, TiN, InO_x , and Be, [5, 15, 17, 19], the low-temperature activated behavior, $R(T) \propto \exp(T_0/T)$ transforms into a variable range hopping upon increasing temperature, contrary to common wisdom expectations. The fact that the high-temperature behavior of the last superconducting sample, S1, is close to that of I2 [$R(T)$ s are nearly indistinguishable at high temperatures; see Fig. 1] evidences the insulating features of superconducting samples in the critical region. On the other hand, the similarity in $R(T)$ between superconducting and insulating samples in the ES regime indicates the presence of Cooper pairs in the insulating samples as well. Further, all these materials exhibit positive magnetoresistance on the insulating side of the D-SIT (InO_x [16] and Be films [20, 21]). And, finally, nonmonotonic dependencies of $T_0(B)$, extracted from the Arrhenius behavior of $R(T)$, and those of the threshold voltage, $V_T(B)$, which we find at the insulating side of D-SIT, have also been observed in the magnetic-field-induced insulating phase in samples, which are superconductors at zero B [5, 6].

We would like to emphasize that the investigated films are homogeneously disordered and do not possess structural granularity. A positive magnetoresistance and threshold behavior, recently reported by [22], were observed in *structurally granular* systems at temperatures where granules are superconducting, while disappearing with the breakdown of superconductivity in granules.

From all the above we conclude that in the critical region of the transition a peculiar highly inhomogeneous insulating phase with superconducting correlations, a *Cooper-pair insulator*, forms. In other words, the films in the critical region may be regarded as possessing a self-induced granularity due to strong mesoscopic fluctuations in disordered superconducting thin films [23] giving rise to formation of superconducting droplets (islands) immersed into an insulating matrix. Such a state can be viewed as a network of superconducting islands coupled by weak links (Josephson junctions arrays). This is strongly supported by experiments of [24], where the voltage threshold similar to ours was observed on the long chains of SQUIDS.

The Cooper-pair insulator establishes as a result of the mutual Josephson phase locking and exhibits generic collective behavior [25]. At moderate temperatures, it shows thermally activated conductivity governed by the large collective Coulomb blockade gap for a Cooper-pair propagation. The observed voltage threshold behavior suggests that the Cooper-pair insulator falls, at very low temperatures, into a distinct *zero-conductivity state*. A nonmonotonic magnetic-field dependence of T_0 and V_T (Fig. 3) naturally results from the magnetic-field modulation of the effective Josephson energy [25, 26]. The appealing task now is the construction of the phase di-

agram of the zero-conductivity state and revealing the mechanisms of depinning and temperature crossovers.

We thank D. Weiss and W. Wegscheider for access to their high magnetic field system, V.F. Gantmakher, M. Feigel'man, A. Finkelstein, and M. Fistul for useful discussions. This research is supported by the Program "Quantum macrophysics" of the Russian Academy of Sciences, the Russian Foundation for Basic Research (Grants No. 06-02-16704 and No. 07-02-00310), the U.S. Department of Energy Office of Science under the Contract No. DE-AC02-06CH11357, and the Deutsche Forschungsgemeinschaft within the GRK 638.

-
- [1] M.P.A. Fisher and D.H. Lee, Phys. Rev. B **39**, 2756 (1989).
 - [2] For a review, see, e.g., A. Goldman and N. Markovic, Physics Today **51**, No. 11, 39 (1998).
 - [3] D.B. Haviland *et al.*, Phys. Rev. Lett. **62**, 2180 (1989); Y. Liu *et al.*, Phys. Rev. B **47**, 5931 (1993).
 - [4] A.F. Hebard and M.A. Paalanen, Phys. Rev. Lett. **65**, 927 (1990).
 - [5] G. Sambandamurthy, L.W. Engel, A. Johansson, and D. Shahar, Phys. Rev. Lett. **92**, 107005 (2004).
 - [6] G. Sambandamurthy, L.W. Engel, A. Johansson, E. Peled, D. Shahar, Phys. Rev. Lett. **94**, 017003 (2005).
 - [7] T.I. Baturina *et al.*, Pis'ma v ZhETF **79**, 416 (2004) [JETP Lett. **79**, 337 (2004)].
 - [8] A. Satta *et al.*, Mat. Res. Soc. Symp. Proc. **612**, D6.5 (2000).
 - [9] see e.g. H.M. Jaeger *et al.*, Phys. Rev. B **40**, 182 (1989); A. Frydman *et al.*, Phys. Rev. B **66**, 052509 (2002).
 - [10] B.I. Shklovskii and A.L. Efros, *Electronic Properties of Doped Semiconductors* (Springer-Verlag, Berlin, 1984).
 - [11] A.L. Efros and B.I. Shklovskii, J. Phys. C **8**, L49 (1975).
 - [12] T.I. Baturina *et al.*, Phys. Rev. Lett. **98**, 127003 (2007).
 - [13] S. Okuma *et al.*, Phys. Rev. B **58**, 2816 (1998).
 - [14] Y. Qin *et al.*, Phys. Rev. B **73**, 100505(R) (2006).
 - [15] D. Shahar and Z. Ovadyahu, Phys. Rev. B **46**, 10917 (1992).
 - [16] V.F. Gantmakher *et al.*, Zh. Eksp. Teor. Fiz. **109**, 1765 (1996) [JETP **82**, 951 (1996)].
 - [17] E. Bielejec *et al.*, Phys. Rev. Lett. **87**, 036801 (2001).
 - [18] W. Wu and E. Bielejec, cond-mat/051121.
 - [19] D. Kowal and Z. Ovadyahu, Solid State Comm. **90**, 783 (1994).
 - [20] E. Bielejec *et al.*, Phys. Rev. B **63**, 100502(R) (2001).
 - [21] V. Yu. Butko and P.W. Adams, Nature **409**, 161 (2001).
 - [22] C. Christiansen, L.M. Hernandez, A.M. Goldman, Phys. Rev. Lett. **88**, 037004 (2002). K.H. Sarwa B. Tan, K.A. Parendo, A.M. Goldman, cond-mat/0704.0765.
 - [23] M.A. Skvortsov and M.V. Feigel'man, Phys. Rev. Lett. **95**, 057002 (2005).
 - [24] E. Chow, P. Delsing, and D.B. Haviland, Phys. Rev. Lett. **81**, 204 (1998).
 - [25] M.V. Fistul, V.M. Vinokur, and T.I. Baturina, arXiv: 0708.2334.
 - [26] I.S. Beloborodov *et al.*, Phys. Rev. B **74**, 014502 (2006).